

The Roles of ATF3 in Glucose Homeostasis

A TRANSGENIC MOUSE MODEL WITH LIVER DYSFUNCTION AND DEFECTS IN ENDOCRINE PANCREAS*

Received for publication, February 1, 2001, and in revised form, May 22, 2001
Published, JBC Papers in Press, May 22, 2001, DOI 10.1074/jbc.M100986200

Amy E. Allen-Jennings^{‡§¶}, Matthew G. Hartman^{‡§**}, Gary J. Kociba^{‡‡}, and Tsonwin Hai^{‡§¶***}

From the [‡]Department of Molecular and Cellular Biochemistry, [§]Neurobiotechnology Center, [¶]Ohio State Biochemistry Program, ^{**}Molecular, Cellular and Developmental Biology Program, ^{‡‡}Veterinary Biosciences, Ohio State University, Columbus, Ohio 43210

Activating transcription factor 3 (ATF3) is a member of the ATF/cAMP-response element-binding protein family of transcription factors. It is a transcriptional repressor, and the expression of its corresponding gene is induced by stress signals in a variety of tissues, including the liver. In this report, we demonstrate that ATF3 is induced in the pancreas by partial pancreatectomy, streptozotocin treatment, and ischemia coupled with reperfusion. Furthermore, ATF3 is induced in cultured islet cells by oxidative stress. Interestingly, transgenic mice expressing ATF3 in the liver and pancreas under the control of the transthyretin promoter have defects in glucose homeostasis and perinatal lethality. We present evidence that expression of ATF3 in the liver represses the expression of genes encoding gluconeogenic enzymes. Furthermore, expression of ATF3 in the pancreas leads to abnormal endocrine pancreas and reduced numbers of hormone-producing cells. Analyses of embryos indicated that the ATF3 transgene is expressed in the ductal epithelium in the developing pancreas, and the transgenic pancreas has fewer mitotic cells than the non-transgenic counterpart, providing a potential explanation for the reduction of endocrine cells. Because ATF3 is a stress-inducible gene, these mice may represent a model to investigate the molecular mechanisms for some stress-associated diseases.

tion factors (reviewed in Refs. 5–10). Although *ATF3* was isolated from a human library (11), homologous genes from rats and mice with about 95% identity to *ATF3* at the amino acid level have been identified: *LRF-1* in the rat (12) and *LRG-21* (13), *CRG-5* (14), or *TI-241* (15) in the mouse. For the convenience of discussion, we will use the *ATF3* nomenclature in the rest of this report. Overwhelming evidence indicates that *ATF3* is induced by a variety of stress signals, such as in the liver by partial hepatectomy, in the brain by seizure, in the heart by ischemia coupled with reperfusion (ischemia-reperfusion), and in the skin by wounding; in addition, it is induced in cultured cells by UV, ionizing radiation, Fas antibody, lipopolysaccharide, and cytokines (reviewed in Refs. 5, 6). Therefore, *ATF3* is induced in many tissues by a variety of stress signals, suggesting that it is a key regulator in cellular stress responses.

Despite overwhelming evidence indicating that *ATF3* is a stress-inducible gene, the physiological consequence of expressing *ATF3* is not clear. In this report, we demonstrate that *ATF3* is induced in the pancreas by stress signals and that transgenic mice expressing *ATF3* in the liver and pancreas have impaired glucose homeostasis. Because *ATF3* is a stress-inducible gene, these transgenic mice may help to elucidate the roles of gene regulation in stress-associated diseases.

EXPERIMENTAL PROCEDURES

Pancreatic Stress Models—For *in vivo* stress models, male Harlan Sprague-Dawley rats at the age of 7–8 weeks were used, and the procedures were performed at Zivic Laboratories (Pittsburgh, PA). Rats were anesthetized by 2.5% halothane, and pancreatic ischemia-reperfusion injury was induced by occluding the mesenteric artery with an arterial clamp for 1 h followed by the removal of the occlusion to allow reperfusion. 2 h after reperfusion, the rat was sacrificed and the pancreas was immediately collected and frozen on powdered dry ice. For partial pancreatectomy, rats were anesthetized and ~70% of the pancreas was removed as the control sample. At 2 h after partial pancreatectomy, the rat was sacrificed and the remaining pancreas was collected. For streptozotocin treatment, rats were fasted for 24 h and injected intravenously with 0.2–0.3 ml of 50 mM sodium citrate solution (pH 4.5) containing streptozotocin (Sigma Chemical Co.) at 65 mg/kg body weight. Control rats were injected with sodium citrate solution. For *in vitro* stress models, RIN-m rat islet cells (ATCC) or β TC6 mouse islet cells (ATCC) were treated with 100 μ M H₂O₂ for 1 h either in the absence or presence of 40 mM *N*-acetyl-L-cysteine (NAC).

Generation of the *TTR-ATF3* Transgenic Mice—A human *ATF3* open reading frame was inserted into the *StuI* site of pTTRexV3 (16) to generate the construct depicted below in Fig. 2A. Transgenic mice were generated in the FVB/N background, and mice containing the transgene were identified by polymerase chain reaction (PCR) using the upstream primer 5'-GAGTCAGGAAGTATGTGAGGG-3' complementary to the *TTR* intron and the downstream primer 5'-CCGGATCCTTAGCTCTGCAATGTTCTTC-3' complementary to the *ATF3* open reading frame.

RNA Isolation, Northern Blot, and Reverse Transcription Coupled with Polymerase Chain Reaction—Rat pancreata were homogenized in 1 ml of TRIzol (Life Technologies) with a Tekmar Tissuemizer at high

Stress signals elicit a variety of cellular responses. Some responses such as that of heat shock have been demonstrated to be protective (1), whereas others such as inflammatory responses have been demonstrated to be detrimental (2–4). The balance between the protective and detrimental events determines the net outcome. We have been investigating a stress-inducible gene, Activating transcription factor 3 (ATF3).¹ ATF3 is a member of the ATF/cAMP-responsive element binding protein family of basic region-leucine zipper (bZip) transcrip-

* This study was supported by NIEHS08690, and grants from the American Diabetes Association, Central Ohio Diabetes Association, and Central Ohio Cancer Research Associates (to T. H.). The costs of publication of this article were defrayed in part by the payment of page charges. This article must therefore be hereby marked "advertisement" in accordance with 18 U.S.C. Section 1734 solely to indicate this fact.

¶ Current address: Joslin Diabetes Center, Boston, MA 02215.

§§ To whom correspondence should be addressed: Rm. 148, Rightmire Hall, 1060 Carmack Rd., Ohio State University, Columbus, OH 43210. Tel.: 614-292-2910; Fax: 614-292-5379; E-mail: hai.2@osu.edu.

¹ The abbreviations used are: ATF3, activating transcription factor 3; PEPCK, phosphoenolpyruvate carboxykinase; TTR, transthyretin; C/EBP, CAAT/enhancer-binding protein; NAC, *N*-acetyl-L-cysteine; RT-PCR, reverse transcriptase-polymerase chain reaction; bp, base pair(s); GAPDH, glyceraldehyde-3-phosphate dehydrogenase; PBS, phosphate-buffered saline; HA, hemagglutinin; FBP, fructose-1,6-bisphosphatase; TAT, tyrosine aminotransferase; E, embryonic day.

speed. RNA was isolated according to the procedures from the manufacturer with the exception that two (instead of one) TRIzol extractions were carried out. For Northern blot, 50 μ g of total RNA was analyzed on a Duralon-UV membrane (Stratagene) using the indicated probes. 32 P-Labeled DNA probes were prepared by random primer reaction using 50–100 ng of the following DNA fragments: 1) 400 bp of human *ATF3* cDNA, 2) 680 bp of rat *cyclophilin* cDNA, 3) 550 bp of mouse *apoA1* cDNA, 4) 500 bp of mouse *apoAII* cDNA, 5) 1500 bp of mouse *Glut 2* cDNA, 6) 600 bp of rat *tyrosine aminotransferase* cDNA, 7) 1400 bp of mouse *PEPCK* cDNA, 8) 300 bp of mouse *fructose-1,6-bisphosphatase* cDNA generated by reverse transcription coupled with polymerase chain reaction (RT-PCR) using upstream primer 5'-AAGGATCCGC-GATCAAAGCCATCTCGT-3' and downstream primer 5'-CCGAATTCCTCAGAAGGCTCATCAGTAC-3'. For RT-PCR, 5 μ g of total RNA was used to generate cDNA with 0.5 μ g of oligo(dT) (Life Technologies) and reverse transcriptase AMV-RT (Promega). 5% of the resulting cDNA was used in PCR to detect rat *ATF3* and *GAPDH* with the following primers: *ATF3* upstream, 5'-GCTGCCAAGTGTGCAAA-CAAG-3'; downstream, 5'-CAGTTTTCCAATGGCTTCAGG-3'; *GAPDH* upstream, 5'-CCGGATCTGGGAAGCTTGTCAACCG-3', and downstream, 5'-GGCTCGAGGACAGTGTGGCATGGACTG-3'. RNA from cultured islet cells was isolated by TRIzol according to the procedures from the manufacturer, and RT-PCR was carried out as above using the same primers, which work for both rat (RIN-m cell) and mouse (β TC6 cells) samples.

Real-time PCR—Real-time PCR was carried out on the iCycler iQ Real Time PCR detection system (Bio-Rad) using gene-specific probes and primers. The probes were labeled at 5' by 6-carboxy fluorescein as fluorescent reporter and at the 3'-end by tetramethylrhodamine as a quencher. The sequences of the probes and primers are as follows: *ATF3* upstream primer, 5'-CGAAGACTGGAGCAAATGATG-3'; *ATF3* probe, 5'-CATCCAGGCCAGTCTCTGCCTCAG-3'; *GAPDH* upstream primer, 5'-CAACGGGAAGCCCATCA-3'; *GAPDH* downstream primer, 5'-CGGCCTCACCCATT-3'; *GAPDH* probe, 5'-CTTCCAGGAGC-GAGACCCCACTAAC-3'. Due to sequence conservation, these primers and probes work for mRNAs derived from both mouse (β TC) and rat (RIN-m) cells. For *ATF3* downstream primer, different sequences were used for mouse and rat: mouse, 5'-CAGGTTAGCAAATCCTCAAATAC-3'; rat, 5'-CAGGTTAGCAAATCCTCAAACAC-3'. The specificity of the primers was tested under normal PCR conditions. Reverse transcription was carried out using 10 μ g of total RNA in 20 μ l of reaction. 5% of the cDNA product was used in Real-time PCR in 25 μ l of reaction. Duplicates or triplicates of PCR were carried out as follows: (a) 95 °C for 3 min, one cycle, (b) 95 °C for 30 s followed by 60 °C for 30 s, 40 cycles. Standard curves were generated using serial dilutions of a plasmid containing the *ATF3* or *GAPDH* cDNA.

Immunohistochemistry—Paraffin sections (4 μ m) on slides were deparaffinized in xylene (10 min, twice), and rehydrated in a decreasing ethanol series diluted in distilled water (100%, 100%, 95%, 95%, 75%, 0%, 5 min each). Endogenous peroxidase activity was inactivated by 0.3% hydrogen peroxide in methanol for 30 min. Sections were blocked with 10% normal goat serum (Vector Laboratories) in a 0.1% Nonidet P-40/PBS solution for 30–60 min and incubated with primary antibody diluted in the blocking solution for overnight at 4 °C in a humidity chamber, unless indicated otherwise (see modifications below). The primary antibodies and dilutions were as follows: rabbit anti-ATF3 (Santa Cruz) at 1:100, guinea pig anti-insulin (Dako) at 1:100, mouse anti-glucagon (Sigma) at 1:1600, rabbit anti-somatostatin (Dako) at 1:200, rabbit anti-pancreatic peptide (Dako) at 1:500, rabbit anti-PDX1 (a gift from C. Wright) at 1:25, rabbit anti-Nkx6.1 (a gift from O. D. Madsen) at 1:3000, and rabbit anti-phospho-histone H3 (Upstate) at 1:200. For some primary antibodies, the following modifications were included. Detection of phospho-histone H3 required an antigen retrieval step (Vector) prior to the hydrogen peroxide step. Detection of PDX-1 and Nkx6.1 also required this antigen retrieval step; in addition, the primary antibodies were incubated with the sections at room temperature for 1 h in a humidity chamber (instead of overnight at 4 °C). Detection of insulin in E12.5 embryos required the following modifications: sucrose frozen sections (instead of paraffin sections) were used, and the blocking solution was 10% normal goat serum with the addition of 2% (w/v) blocking powder (Roche Molecular Biochemicals); in addition, the primary antibodies were incubated with the sections at room temperature for overnight. After incubating with the primary antibodies as described above, the sections were washed and incubated with a biotinylated secondary antibody, followed by incubation with the ABC elite reagent (containing avidin-conjugated peroxidase) and color reaction using the DAB substrate kit according to the recommendation from the manufacturer (Vector Laboratories). After the color reaction, sec-

tions were dehydrated through an ethanol series into xylene and mounted using Permount mounting media (Fisher Scientific). For some sections, counterstain with methyl green (Vector Laboratories) or hematoxylin and eosin (H&E) (Richard Allen) prior to dehydration was carried out to help visualize the tissue morphology.

Area Measurement and Quantification of Immunohistochemistry Signals—The area measurement was carried out using the Bioquant Nova, Image Analysis System, version 4.00.8, (R and M Biometrics, Nashville, TN). For quantification of immunohistochemistry signals, investigators blind to the genotypes counted the signals from multiple samples and normalized them against the area.

Preparation and Staining of Tissue Sections—Newborn mice were sacrificed by decapitation; tissues were removed and rinsed in ice-cold phosphate buffer saline (PBS). For samples from embryos, the appearance of a vaginal plug was considered day 0.5 of gestation. Embryos from time pregnant females were removed at the indicated gestation time and dissected in ice-cold PBS. Tissues or embryos were fixed for 1–3 days in 10% phosphate-buffered formalin, pH 7.0 (Fisher Scientific), at 4 °C. Paraffin sections were prepared and stained by H&E at the Ohio State University Veterinary Histology Laboratory.

Collection of Sera and Serum Glucose Assay—Mice were decapitated with scissors, and the blood was immediately collected in micro-hematocrit capillary tubes (Fisher Scientific) and transferred to Microtainer serum separator tubes (Beckton Dickinson). The tubes were centrifuged according to the instruction from the manufacturer, and the top layer (serum) was analyzed on the same day or after storage at –20 °C. Serum glucose concentrations were determined using the hexokinase method (Roche Molecular Biochemicals). For samples with size less than 5 μ l, analyses were run on a Kodak Ektachem DT60 II analyzer at the Ohio State University Veterinary Histology Laboratory.

RESULTS

Induction of ATF3 in the Pancreas by Stress Signals—To find out whether *ATF3* is induced in the pancreas by stress signals, we examined its expression in three pancreatic stress models: partial pancreatectomy, ischemia-reperfusion, and streptozotocin treatment (see "Discussion"). As shown by RT-PCR, the level of *ATF3* mRNA greatly increased at 2 h after induction in all three stress models (Fig. 1A). However, the level of a control mRNA *glyceraldehyde-3-phosphate dehydrogenase (GAPDH)* did not change. The specificity of the signal was indicated by the lack of signal if reverse transcriptase was omitted in the reaction (data not shown). Therefore, *ATF3* is induced in the pancreas by stress signals. To test whether *ATF3* is also induced *in vitro*, we examined the induction of *ATF3* in RIN-m and β TC6 islet cells. Because one potential mechanism for the induction of *ATF3* by stress signals is oxidative stress, we used H_2O_2 as a stressor in the *in vitro* experiments. As shown in Fig. 1B, *ATF3* mRNA increased at 1 h after H_2O_2 treatment. Real-time PCR analysis indicated that the induction was about 13-fold in RIN-m cells and 5-fold in β TC6 cells. Significantly, *N*-acetyl-L-cysteine (NAC), an antioxidant scavenger (17, 18), greatly reduced the induction, suggesting that H_2O_2 induces *ATF3* through an oxidative stress-mediated mechanism. Taken together, these results indicate that *ATF3* is induced by stress signals in the pancreas and in cultured islet cells, suggesting that it may play an important role in pancreatic stress response.

Generation of the TTR-ATF3 Transgenic Mice—One common theme of the signals that induce *ATF3* is that they all induce cellular damage. This correlation, however, does not indicate whether the induction of *ATF3* is a beneficial or detrimental stress response. To address this question, we took a gain-of-function approach. We generated transgenic mice expressing *ATF3* under the control of the *transferrin (TTR)* promoter, a promoter that is predominantly active in the liver and choroid plexus (16, 19, 20) but could also be active in the endocrine pancreas (21). Fig. 2A shows the transgenic construct, and for the convenience of discussion, we will refer to these mice as TTR-ATF3 mice. Thus far, we have generated 24 transgenic founders, and for reasons unknown, these founders did not

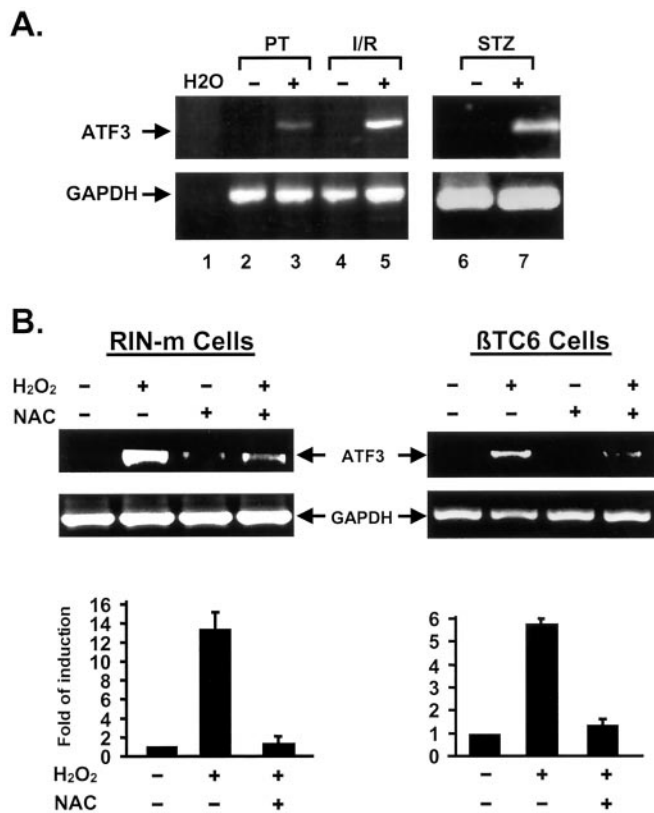


FIG. 1. *ATF3* was induced in the pancreatic cells by stress signals *in vivo* and *in vitro*. *A*, rats were treated with mesentery artery occlusion for 1 h followed by the release of the occlusion for 2 h to induce ischemia-reperfusion (*I/R*) injury in the pancreas. Pancreas from a sham-operated rat was collected as a control sample (–). For partial pancreatectomy (*PT*), 70% of the pancreas was removed as a control sample (–), and the remaining pancreas was collected at 2 h after treatment. Total RNA isolated from the pancreas was analyzed by RT-PCR to detect *ATF3* and *GAPDH* mRNAs. Lane 1 shows a water control for PCR, where water was used to replace cDNA. A representative result from three experiments is shown. *B*, rat RIN-m and mouse β TC6 islet cells were treated with 100 μ M H₂O₂ for 1 h either in the absence or presence of 40 mM NAC as indicated. Total RNA was isolated and analyzed by RT-PCR or RT coupled with real-time PCR. *ATF3* transcripts quantified from real-time PCR were normalized against *GAPDH* transcripts, and the normalized signals in uninduced cells were arbitrarily defined as 1. Data represent mean \pm S.E. from three independent experiments.

express detectable levels of the *ATF3* transgene. However, they could pass on the transgene to their progeny, and the F1 progeny expressed the *ATF3* transgene in the liver as indicated by immunohistochemistry (Fig. 2*B*). Similar results were obtained using antibodies against the hemagglutinin (HA) tag, which is specific to the transgene. By *in situ* hybridization, the transgenic mRNA was detectable in the developing liver starting at embryonic day 12.5 (E12.5) (data not shown). Northern blot analysis indicated that the level of expression in F1 mice from different founders was comparable, and one example is shown in Fig. 3. Consistent with the previous report that the *TTR* promoter could be active in the pancreas (21), the transgene was also expressed in the pancreas, specifically in the ductal epithelium, as shown by immunohistochemistry using *ATF3* antibody (Fig. 2*B*) or HA antibody (data not shown). However, this pancreatic expression was detected in F1 mice derived from some but not all founders (more detail below), presumably due to the differences in the integration sites or copy numbers.

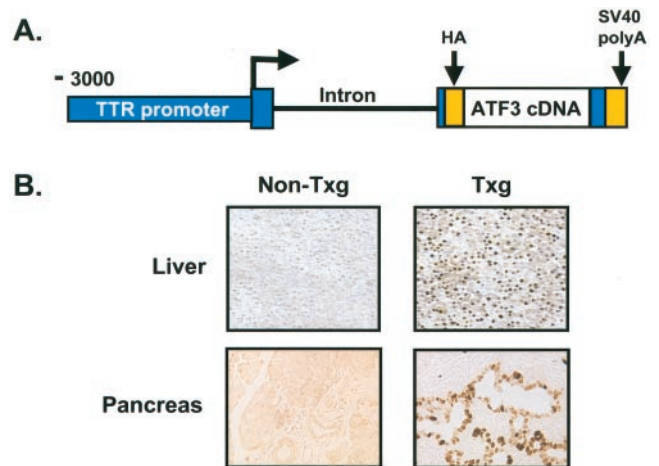


FIG. 2. Expression of *ATF3* in the TTR-*ATF3* transgenic mice. *A*, a schematic of the TTR-*ATF3* construct. Filled boxes indicate the promoter and non-coding exons of the *TTR* gene. HA, hemagglutinin tag. *B*, liver or pancreas sections from postnatal day 7 (P7) transgenic (*Txg*) or non-transgenic (*Non-Txg*) mice were analyzed by immunohistochemistry using antibodies against *ATF3*. Magnification, \times 400.

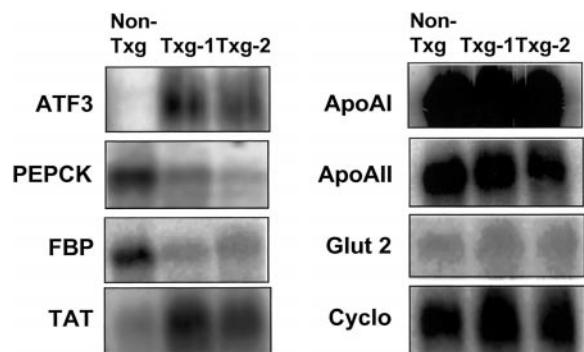


FIG. 3. Transgenic livers had altered steady-state mRNA levels for genes encoding key gluconeogenic enzymes. Total RNAs (50 μ g) from livers of transgenic (*Txg*) and non-transgenic (*Non-Txg*) mice at the age of P1 to P7 were analyzed by Northern blot for the following mRNAs: *ATF3*, phosphoenolpyruvate carboxykinase (*PEPCK*), fructose-1,6-bisphosphatase (*FBP*), tyrosine aminotransferase (*TAT*), apolipoprotein A1 (*apoA1*), apolipoprotein AII (*apoAII*), glucose transporter 2 (*Glut 2*), and cyclophilin (*Cyclo*), which served as a loading control. *Txg-1* and *Txg-2* represent transgenic mice derived from two different founders. To quantify the signals, we normalized each signal against cyclophilin and arbitrarily defined the normalized signals from non-transgenic mice as 1. The followings are mean \pm S.E. from five to eight experiments: *PEPCK*, 0.33 \pm 0.08; *FBP*, 0.25 \pm 0.06; *TAT*, 3.5 \pm 0.5; *apoA1*, 0.9 \pm 0.8; *apoAII*, 1.6 \pm 0.2; *Glut 2*, 1 \pm 0.6. Shown is one representative result.

Perinatal Death of the TTR-*ATF3* Mice—All TTR-*ATF3* mice (F1 progeny) had growth retardation. This phenotype was observed in F1 mice derived from all 24 founders, indicating that it was due to the transgene rather than the sites of integration. Most of these F1 mice died between 30 min to a few hours after birth. To facilitate the analyses, we crossed the founders (FVB/N mice) with wild type BALB/c mice to generate the “F1 hybrid.” These F1 mice had the advantage of hybrid vigor and survived longer. Most of them died within 4 days, and some survived for up to 7 days. Because the F1 hybrid mice are genetically uniform except at the locus containing the transgene, comparison of the transgenic mice with the non-transgenic littermates allowed us to assess the consequences of expressing *ATF3*. Although the founders were viable, several factors made it difficult to carry out detailed analyses of F1 mice from all founders. First, some founders appeared to have low fertility, because they rarely gave rise to progeny despite continuous mating. Second, the transgenic transmission rate for most founders was less than 50%, the expected rate for the

cross between transgenic founders and non-transgenic mice. Third, some founders died within a few months. Because of these difficulties, detailed analyses were carried out using mice derived from some but not all founders. Results described below were reproducibly observed from multiple founders.

Altered Expression of Genes Encoding Gluconeogenic Enzymes—During the perinatal period, newborns need to elicit a series of adaptations to maintain glucose homeostasis (22). To investigate whether the transgenic livers have impaired gluconeogenesis, we examined the expression of genes encoding phosphoenolpyruvate carboxykinase (PEPCK) and fructose-1,6-bisphosphatase (FBP), two rate-limiting enzymes of gluconeogenesis. As shown by Northern blot analysis, the levels of *PEPCK* and *FBP* mRNAs were lower in the transgenic livers than those in the non-transgenic livers (Fig. 3). This reduction was observed in all F1 mice examined thus far. The control *cyclophilin* mRNA levels were similar, suggesting that the difference was not due to a difference in the amount of RNA analyzed. Importantly, the transgenic livers had detectable levels of *ATF3* mRNA, but the non-transgenic livers did not. The level of *ATF3* mRNA in all transgenic livers examined thus far was similar, and Fig. 3 shows an example comparing two F1 mice (Txg-1 and Txg-2) derived from different founders. We also examined the expression of several other hepatic genes and found no obvious difference between transgenic and non-transgenic livers: *apoA1*, *apoAII*, and *Glut 2*. Interestingly, the level of *tyrosine aminotransferase (TAT)* mRNA was higher in the transgenic than that in the non-transgenic livers. The implication of this increase is discussed (see below).

Abnormal Endocrine Pancreas—As described above, F1 mice derived from some of the founders also expressed the transgene in the pancreas. These mice had pancreas defects, although the defects varied in the degrees of their severity. In mice with severe defects, the pancreas lacked islets of Langerhans completely (Fig. 4A). Analysis of serial sections spanning the entire pancreas from six mice showed no islets in any section. In mice with mild defects, the pancreas lacked islets of Langerhans in some but not all serial sections (data not shown). This is in contrast to the non-transgenic mice, in which islets were observed in all pancreatic sections examined. Immunohistochemistry analysis indicated that the islets in these transgenic pancreata had an abnormal distribution of hormone-producing cells. In contrast to its normal location in the center of the islets, insulin-producing (ins^+) cells were located in the periphery of the islets and scattered outside (Fig. 4B). In addition, clusters of glucagon-producing (glu^+) cells scattered outside the islets (Fig. 4B).

The variation in the severity of pancreas defects was founder-specific; that is, founders giving rise to F1 mice with severe pancreas defects invariably gave rise to mice with severe pancreas defects, and the same was true for the case of mild pancreas defects. Varying degrees in the severity of phenotypes are commonly observed in transgenic work, and one potential explanation for the variation is the level or pattern of transgene expression. Table I compares the expression of *ATF3* in F1 mice derived from six founders. Because *ATF3* is expressed in only a subset of pancreatic cells, we examined the pancreas by immunohistochemistry instead of Western blot. Although immunohistochemistry is not a quantitative assay, we consistently observed differences in the intensity of the signals. Samples derived from #90 progeny gave strong signals within minutes after incubation with the substrates, and an example is shown in Fig. 2B. Samples derived from #4 and #72 progeny never gave any detectable signals even after a prolonged incubation. Samples derived from #28 and #43 progeny gave detectable signals; however, it required a long incubation with the

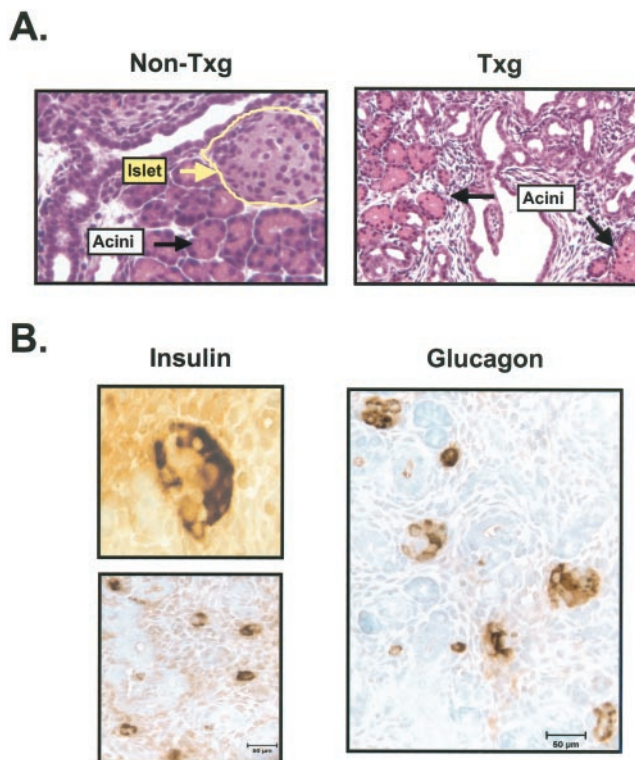


FIG. 4. **Transgenic mice had abnormal endocrine pancreas.** A, F1 mice derived from founder 90 lacked islets of Langerhans. Pancreas sections from a P4 transgenic mouse (*Txg*) and its non-transgenic littermate (*Non-Txg*) were stained with H&E. Islets of Langerhans and acini (exocrine cells) are indicated. Magnification, $\times 400$. B, F1 mice derived from founder 43 had abnormal distribution of hormone-producing cells. Pancreas sections from a P4 transgenic mouse (*Txg*) and its non-transgenic littermate (*Non-Txg*) were analyzed by immunohistochemistry using antibodies against insulin or glucagon as indicated. Bar, $\times 400$.

TABLE I
Comparison of F1 mice derived from six founders

The expression of *ATF3* was examined by immunohistochemistry, and the level is defined as strong ($++$), medium ($+$), weak (\pm), or none ($-$) as detailed in the text. Pancreas morphology was examined by H&E stain. Severe phenotype is defined as no islets of Langerhans in any serial sections examined spanning the entire pancreas. Mild phenotype is defined as lack of islets in some but not all serial sections. These islets had abnormal organization of the hormone-producing cells as shown in Fig. 4B. Serum glucose level is defined as high (387 ± 51 mg/dl), normal to high (ranged from 150 to 350 mg/dl), normal (similar to non-transgenic mice, which had 128 ± 26 mg/dl), and low (64 ± 7 mg/dl).

Founder number	<i>ATF3</i> level in pancreas	Pancreas defects (by morphology)	Serum glucose
90	$++$	Severe	High
28	$+$	Mild	Normal to high
43	$+$	Mild	Normal
34	\pm	Normal	Normal
4	$-$	Normal	Low
72	$-$	Normal	Low

substrate. We note that the expression pattern in these mice was also different from that from #90 progeny (shown in Fig. 2B). In addition to the ductal expression, *ATF3*-expressing cells were found in the islets and scattered outside (data not shown). On the basis of the signal intensity, we assigned the levels of *ATF3* expression as strong ($++$), medium ($+$), weak (\pm) or none ($-$). As shown in Table I, a general trend exists: The stronger the *ATF3* expression, the more severe the pancreas defects.

Disturbance in Glucose Homeostasis—Because both liver and pancreas play a role in glucose homeostasis, we compared the serum glucose levels of the F1 transgenic mice with that of the

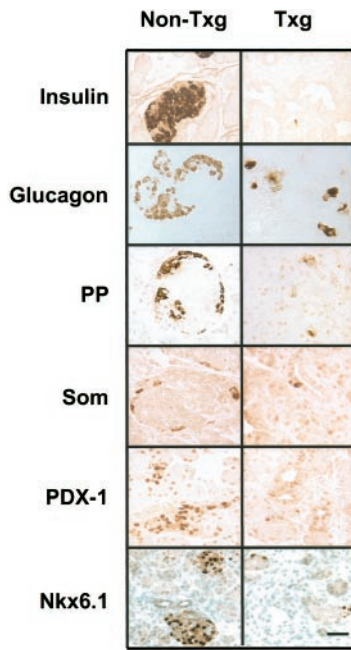


FIG. 5. Transgenic mice had fewer endocrine cells than the non-transgenic mice. Pancreatic sections from P1–P7 transgenic (*Txg*) or non-transgenic (*Non-Txg*) mice were examined by immunohistochemistry using the indicated antibodies: insulin, glucagon, pancreatic peptide (*PP*), somatostatin (*Som*), PDX-1, and Nkx6.1. Bar, 20 μ m.

non-transgenic littermates. As shown in Table I, F1 mice from founders 4 and 72 had low serum glucose levels when compared with the non-transgenic mice. One explanation for this result is that the transgenic mice had reduced gluconeogenic activity in the liver due to the reduced expression of *PEPCK* and *FBP* as shown in Fig. 3, resulting in lower glucose levels in the serum. However, despite the reduced *PEPCK* and *FBP* expression in all F1 mice as described above, mice from founder 90 had high serum glucose levels. One explanation is that these mice had severe pancreas defects, resulting in significantly reduced ins^+ cells (Fig. 5). In this case, the pancreas phenotype predominates, resulting in high serum glucose level. Taken together, results shown in Table I are consistent with the interpretation that the relative severity of the defects in the pancreas *versus* the liver determined the serum glucose level.

Reduction in All Four Endocrine-producing Cells—The islet of Langerhans contains four types of endocrine cells: glu^+ , ins^+ , somatostatin-producing (som^+), and pancreatic peptide-producing (PP^+) cells. These cells are scattered as individual clusters during early development and become aggregated to form organized islets at late gestation (reviewed in Refs. 23, 24, 25–27). To examine whether the lack of islets shown in Fig. 4 was due to the lack of endocrine cells, we examined the pancreas by immunohistochemistry using antibodies against each hormone: glucagon, insulin, somatostatin (*Som*), and pancreatic peptide (*PP*). As shown in Fig. 5, all four endocrine cells were reduced in the transgenic mice (derived from founder 90). Although the transgenic mice had reduced ins^+ cells, they might still have “presumptive β cells” but fail to synthesize insulin. Therefore, we examined the expression of *PDX-1* and *Nkx6.1*, two transcription factors with restricted expression in mature β cells (28–31). As shown in Fig. 5, both *PDX-1*- and *Nkx6.1*-producing cells were dramatically reduced, suggesting that the transgenic mice lack β cells.

Potential Explanations for the Pancreatic Defects—Because mice derived from founder 90 had the most severe pancreas phenotype, we further analyzed them. The following observations indicate that the defects are most likely due to the ex-

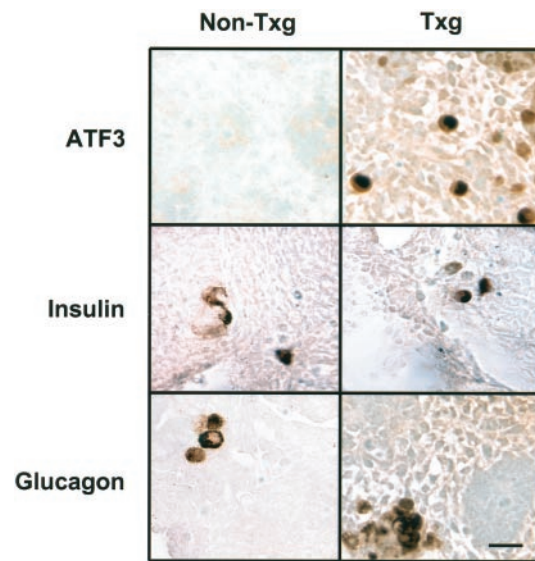


FIG. 6. E12.5 transgenic embryos expressed the *ATF3* transgene but still had insulin- and glucagon-producing cells. Sections containing the pancreatic primordium from transgenic (*Txg*) or non-transgenic (*Non-Txg*) embryos at E12.5 were examined by immunohistochemistry using the indicated antibodies: ATF3, insulin, glucagon. Bar, 20 μ m.

pression of the *ATF3* transgene. First, *ATF3* was expressed in the right place: It was expressed in the pancreatic ducts (Figs. 2B) where the precursor cells originate (reviewed in Refs. 24, 25–27). Second, *ATF3* was expressed at the right time: Its expression was detectable starting at E12.5 (Fig. 6), a critical time for endocrine precursors to differentiate (reviewed in Refs. 25–27, 32). Significantly, the differences between the transgenic and non-transgenic embryos became apparent shortly after *ATF3* was detectable. At E14.5, the numbers of ins^+ and glu^+ cells were obviously lower in transgenic mice than those in non-transgenic mice; Fig. 7 shows a representative picture. To quantify the difference, investigators blind to the genotypes counted positive cells in sagittal sections close to the midline, where the pancreatic primordium can be easily identified (33) as shown by the *dotted line* in Fig. 8B. The signals were then standardized against the area obtained from a computer-assisted area measurement. Results from multiple sections indicated that the transgenic pancreatic primordium had ~80% fewer ins^+ cells and 45% fewer glu^+ cells, when compared with the non-transgenic counterpart. The reduction for glu^+ cells was not as dramatic as that for ins^+ cells. This was also observed in embryos at later gestation (E16.5, E18.5, data not shown) and in newborn mice (Fig. 5). We note that the exocrine cells had no obvious defects as shown by morphological analysis and immunohistochemistry assay using antibody against amylase, an exocrine marker (data not shown). It is not clear why exocrine cells were not affected, because they are also derived from ductal epithelium. It is possible that transgenic mice had subtle defects in their acini, but the defects were not detected by the assays used thus far.

One potential mechanism for the reduced endocrine cells is the reduction of cell proliferation. To test this possibility, we examined the pancreatic primordium by immunohistochemistry using an antibody against phospho-histone H3, a mitotic marker (34, 35). As shown in Fig. 8A, in both transgenic and non-transgenic pancreatic primordia at E14.5, mitotic cells were present within or near the ductal epithelium. This is consistent with previous observations that undifferentiated precursor cells located in the ducts have the highest proliferative capacity (see “Discussion”). To determine whether the mi-

otic index is different in transgenic and non-transgenic embryos, we quantified the signals as described above. Results from multiple sections indicated that the transgenic pancreatic primordium had fewer ($30 \pm 1\%$) mitotic cells than the non-transgenic counterpart. Fig. 8C shows a representative picture counterstained by methyl green, which provides a clear contrast to the *dark brown* signals. A low magnification was used to show a large area of the pancreatic primordium. We note that the intensity of the signal was consistently lower in the transgenic mice than that in the non-transgenic mice.

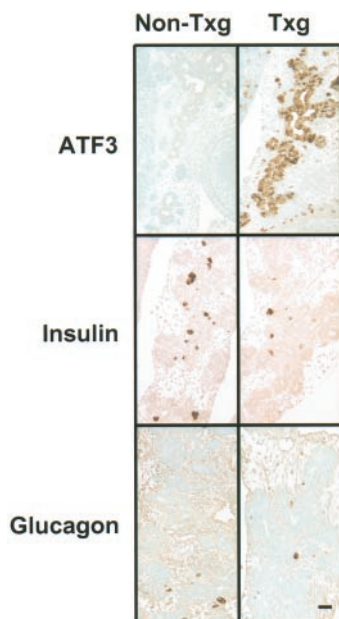


FIG. 7. E14.5 transgenic embryos expressed the *ATF3* transgene and had fewer insulin- and glucagon-producing cells than the non-transgenic embryos. Sections containing the pancreatic primordium from transgenic (*Txg*) or non-transgenic (*Non-Txg*) embryos at E14.5 were examined by immunohistochemistry using the indicated antibodies: ATF3, insulin, glucagon. Low magnification was used to generate this figure to show a large area of the pancreatic primordium. Bar, 20 μ m.

DISCUSSION

***ATF3* Expression in the Liver Affects Gluconeogenesis**—As described in the introduction, *ATF3* is induced in the liver by many stress signals. In this report, we demonstrate that the *TTR-ATF3* transgenic mice had reduced steady-state mRNA levels of *PEPCK* and *FBP*. Because *PEPCK* and *FBP* encode enzymes that catalyze two rate-limiting steps of gluconeogenesis, our results are consistent with a model that gluconeogenesis was reduced in the mice. Interestingly, both *PEPCK* and *FBP* promoters contain ATF/CRE or ATF/CRE-like sites (reviewed in Refs. 36, 37 and references therein, 38). Because *ATF3* is a transcriptional repressor (39), it is possible that *ATF3* inhibits the activity of these promoters, resulting in reduced mRNA levels in the transgenic mice. As shown in Fig. 3, the steady-state mRNA levels of *TAT*, which encode another gluconeogenic gene, was higher in the transgenic mice than those in the non-transgenic mice. Similar to *PEPCK*, the expression of *TAT* is up-regulated by the cAMP and glucocorticoid signaling pathways (for an example, see Ref. 40). Therefore, the increase in *TAT* mRNA levels in the transgenic mice suggests that the mice could respond properly to cAMP and glucocorticoid signaling. This in turn suggests that the defects in *PEPCK* gene expression in the transgenic mice were due to events downstream from the signaling pathways.

Disturbance of Glucose Homeostasis in the TTR-ATF3 Transgenic Mice—In this report, we showed that the *TTR-ATF3* transgenic mice had defects in two organs important for regulating serum glucose levels: liver and pancreas. As described above, expression in the liver would contribute to reduced gluconeogenesis and reduced serum glucose level. Our results indicate that expression in the pancreas led to an abnormal endocrine pancreas: either reduced islets of Langerhans (mild phenotype) or a complete lack of islets (severe phenotype). These defects would contribute to high serum glucose. Presumably, the relative severity of the defects in these two organs determined the serum glucose level. As described under “Results,” the variation in the severity of the pancreas phenotype was founder-specific. Founders that gave rise to F1 mice with mild phenotype always gave rise to mice with mild phenotype, and the same was true for the severe phenotype. One possibility for this difference is the difference in the level of transgene

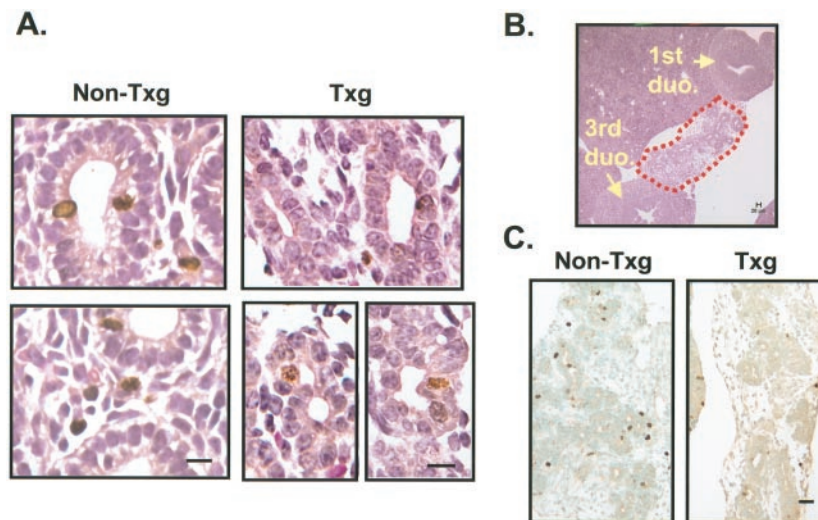


FIG. 8. E14.5 pancreatic primordium had fewer mitotic cells in the transgenic embryos than that in the non-transgenic embryos. A, sections containing the pancreatic primordium from transgenic (*Txg*) or non-transgenic (*Non-Txg*) embryos at E14.5 were examined by immunohistochemistry using antibodies against phospho-histone H3, a mitotic marker, followed by counter-stain with H&E. Bar, 20 μ m. B, a sagittal section close to the midline of a non-transgenic embryo stained with H&E is shown to indicate the pancreatic primordium (delineated by the dotted line), which is between the first part of the duodenum (*1st duo.*) and the third part of the duodenum (*3rd duo.*) (33). Bar, 20 μ m. C, same as A except the counterstain was carried out using methyl green, which provides a better contrast to the signal (*dark brown*) than the H&E stain. In addition, a lower magnification was used to show a larger field than that shown in A. Bar, 20 μ m.

expression (in the pancreas). As indicated in Table I, immunohistochemistry showed a good correlation between transgene expression and the degree of severity: The stronger the expression in the pancreas, the stronger the pancreas defects. We note that F1 mice derived from founder 34 had faint signals of *ATF3* expression in the pancreas but had no obvious defects. It is possible that the pancreas had minor defects that were not detected by the analyses used. At present, it is not clear whether the timing for turning on the transgene in the pancreas was different in mice from different founders. Presumably, a difference here would also lead to variations in the phenotype.

The Roles of *ATF3* in Pancreatic Stress Response—As shown in this report, *ATF3* is induced in three important pancreatic stress models: partial pancreatectomy, streptozotocin treatment, and ischemia-reperfusion. Partial pancreatectomy leads to an initial burst of pancreatic regeneration followed by chronic hyperglycemia (41) and is considered as a model of β cell adaptation to injury (42). Streptozotocin is a commonly used agent to induce experimental diabetes in animals, because it selectively destroys β cells (43). Ischemia-reperfusion injury is involved in the pathophysiology of acute pancreatitis and tissue injury after pancreas transplantation (44, 45). Therefore, all three models used in this study are considered to be important pancreatic stress models. In addition to animal models, we demonstrated that *ATF3* was induced in cultured islet cells by H_2O_2 , an agent that has been demonstrated to induce β cell injury and has been used as a paradigm for studying the roles of oxidative stress in the pathogenesis of diabetes and pancreatitis (for reviews, see Refs. 46–48). Significantly, our results suggest that H_2O_2 induces *ATF3* through an oxidative stress-mediated pathway, because NAC, an agent that has been demonstrated to scavenge oxidants (17) and increase intracellular glutathione levels (18), greatly inhibited the ability of H_2O_2 to induce *ATF3*. We note that an oxidative stress-mediated pathway has been implicated in both ischemia-reperfusion and streptozotocin-induced cellular damages (for some examples, see Refs. 49–51). Therefore, both *in vivo* and *in vitro* results suggest that oxidative stress may be a common element in the induction of *ATF3* by stress signals.

Regulation of gene expression has been postulated to be important for β cell function and the development of diabetes. Weir *et al.* (52) hypothesized that a set of transcription factors maintains the differentiation of β cells and that disturbance of this unique gene expression pattern leads to diabetes. In support of this hypothesis, they demonstrated that the expression of many genes important for β cell development and differentiation is altered in an animal model of diabetes (53). Our results further support this hypothesis. Because *ATF3* is a transcription factor, ectopic expression of *ATF3* undoubtedly perturbs gene expression. Although we have not identified the target genes for *ATF3* in the pancreas, the phenotypes we observed in the transgenic mice further strengthen the notion that altered gene expression can lead to β cell dysfunction.

Reduced Mitotic Index in the Transgenic Mice—As described above, the pancreatic primordium had fewer mitotic cells in the transgenic than in the non-transgenic embryos. In this study, we examined mitosis by using antibody against phospho-histone H3, because the phosphorylation of histone H3 is M-phase-specific (34, 35). We note that most of the mitotic cells are located either within or near the ductal epithelium. This is consistent with the current understanding of islet cell expansion. Islet cell expansion can be achieved by either proliferation of the pre-existing, differentiated islet cells (a process called replication), or proliferation of undifferentiated precursor cells located in the ducts (a process called neogenesis) (reviewed in

Refs. 24, 54–56). Studies in both human and rodent embryos indicate that neogenesis plays the major role in islet expansion, because undifferentiated ductal precursors have much higher proliferative capacity than the differentiated endocrine cells (57–60, reviewed in Refs. 55, 56). Therefore, our results of mitotic cells located within or near the ductal epithelium are consistent with previous observations. Fig. 8A is a composite of several fields, because the number of mitotic cells in any given field was relatively low. This is because the mitotic phase only accounts for a small percentage of the total cell cycle duration; in pancreatic β cells, it was estimated to be about 3% (56). It is not clear, at present, which cell cycle phase was arrested in the transgenic pancreas to attribute to this low mitotic index.

The finding that transgenic pancreas has a lower mitotic index than the non-transgenic pancreas provides at least one potential explanation for the endocrine pancreas defects we observed. Although *ATF3* is a transcription factor, it is not clear whether the inhibition of cell proliferation observed here is due to its ability to regulate transcription. This is because transcription factors have been demonstrated to affect cell proliferation in a DNA-binding-independent manner. One such example is *C/EBP α* . From a series of elegant work (61–63), Darlington and colleagues demonstrated that *C/EBP α* inhibits cell proliferation not by regulating transcription. Instead, it inhibits cell proliferation by interacting with cell cycle regulatory proteins: cyclin-dependent kinase inhibitor p21 and retinoblastoma-like protein p107. Therefore, the effect of *ATF3* on cell proliferation may not depend on its ability to regulate transcription. Much work is required to elucidate the molecular details and is beyond the scope of this report.

Acknowledgments—We thank Dr. T. Van Dyke for the TTR vector, Drs. G. Darlington and G. Schütz for the FBP, TAT, apoAI, apoAII, and Glut 2 DNAs, Drs. C. Wright and M. Gannon for PDX-1 antibodies and protocol, Dr. O. D. Madsen for Nkx6.1 antibodies, and Dr. B. Sosa-Pineda for the insulin immunohistochemistry protocol and suggestions. We thank Dr. R. Hanson for insightful suggestions and critical comments on the manuscript, Dr. M. Reitman for initial analysis of serum insulin levels and helpful suggestions, Drs. G. Darlington, R. Costa, C. Wright, R. Stein, C. Croniger, and H. Vaessin for helpful comments and discussions. We thank Dr. J. Parker-Thornburg at the KECK Genetic Research Facility, Ohio State University for generating the TTR-*ATF3* mice.

REFERENCES

- Morimoto, R. I., Tissieres, A., and Georgopoulos, C. (1994) *The Biology of Heat Shock Proteins and Molecular Chaperones*, Cold Spring Harbor Laboratory Press, Plainview, NY
- Barnes, P. J. (1999) *Nature* **402**, B31–B38
- Baldwin, A. S., Jr. (1996) *Annu. Rev. Immunol.* **14**, 649–683
- Kyriakis, J. M., and Avruch, J. (1996) *J. Biol. Chem.* **271**, 24313–24316
- Hai, T., Wolfgang, C. D., Marsee, D. K., Allen, A. E., and Sivaprasad, U. (1999) *Gene Expression* **7**, 321–335
- Hai, T., and Hartman, M. G. (2001) *Gene*, in press.
- Brindle, P. K., and Montminy, M. R. (1992) *Curr. Opin. Genet. Dev.* **2**, 199–204
- Meyer, T. E., and Habener, J. F. (1993) *Endocr. Rev.* **14**, 269–290
- Sassone-Corsi, P. (1994) *EMBO J.* **13**, 4717–4728
- Ziff, E. B. (1990) *Trends Genet.* **6**, 69–72
- Hai, T., Liu, F., Coukos, W. J., and Green, M. R. (1989) *Genes Dev.* **3**, 2083–2090
- Hsu, J.-C., Laz, T., Mohn, K. L., and Taub, R. (1991) *Proc. Natl. Acad. Sci. U. S. A.* **88**, 3511–3515
- Drysdale, B.-E., Howard, D. L., and Johnson, R. J. (1996) *Mol. Immunol.* **33**, 989–998
- Farber, J. M. (1992) *Mol. Cell. Biol.* **12**, 1535–1545
- Ishiguro, T., Nakajima, M., Naito, M., Muto, T., and Tsuruo, T. (1996) *Cancer Res.* **56**, 875–879
- Wu, H., Wade, M., Krall, L., Grisham, J., Xiong, Y., and Van Dyke, T. (1996) *Genes Dev.* **10**, 245–260
- Aruoma, O. I., Halliwell, B., Hoey, B. M., and Butler, J. (1989) *Free Radic. Biol. Med.* **6**, 593–597
- Burgunder, J. M., Varriale, A., and Lauterburg, B. H. (1989) *Eur. J. Clin. Pharmacol.* **36**, 127–131
- Yan, C., Costa, R. H., Darnell, J. E., Chen, J. D., and Van Dyke, T. A. (1990) *EMBO J.* **9**, 869–878
- Ye, H., Holterman, A. X., Yoo, K. W., Franks, R. R., and Costa, R. H. (1999) *Mol. Cell. Biol.* **19**, 8570–8580
- Jacobsson, B., Collins, V. P., Grimelius, Pettersson, T., Sandstedt, B., and Carlstrom, C. (1989) *J. Histochem. Cytochem.* **37**, 31–37

22. Girard, J., Ferre, P., Pegorier, J. P., and Duee, P. H. (1992) *Physiol. Rev.* **72**, 507–562
23. Pictet, R. L., Clark, W. R., Williams, R. H., and Rutter, W. J. (1972) *Dev. Biol.* **29**, 436–467
24. Pictet, R., and Rutter, W. J. (1972) in *Handbook of Physiology* (Steiner, D. F., and Frenkel, N., eds) pp. 25–66, Williams & Wilkins, Baltimore, MD
25. Edlund, H. (1998) *Diabetes* **47**, 1817–1823
26. Sander, M., and German, M. S. (1997) *J. Mol. Med.* **75**, 327–340
27. Slack, J. M. W. (1995) *Development* **121**, 1569–1580
28. Ohlsson, H., Karlsson, K., and Edlund, T. (1993) *EMBO J.* **12**, 4251–4259
29. Guz, Y., Montminy, M. R., Stein, R., Leonard, J., Gamer, L. W., Wright, C. V. E., and Teitelman, G. (1995) *Development* **121**, 11–18
30. Øster, A., Jensen, J., Serup, P., Galante, P., Madsen, O. D., and Larsson, L.-I. (1998) *J. Histochem. Cytochem.* **46**, 707–715
31. Jensen, J., Serup, P., Karlsen, C., Nielsen, T. F., and Madsen, O. D. (1996) *J. Biol. Chem.* **271**, 18749–18758
32. Habener, J. F., and Stoffers, D. A. (1997) *Proc. Assoc. Am. Physicians* **110**, 12–21
33. Kaufman, M. H. (1992) *The Atlas of Mouse Development*, Academic Press, London
34. Lake, R. S., and Salzman, N. P. (1972) *Biochemistry* **11**, 4817–4826
35. Gurley, L. R., D'Anna, J. A., Barham, S. S., Deaven, L. L., and Tobey, R. A. (1978) *Eur. J. Biochem.* **84**, 1–15
36. Nizielski, S. E., Lechner, P. S., Croniger, C. M., Wang, N.-D., Darlington, G. J., and Hanson, R. W. (1996) *J. Nutr.* **126**, 2697–2708
37. Granner, D., O'Brien, R., Imai, E., Forest, C., Mitchell, J., and Lucas, P. (1991) *Recent Prog. Horm. Res.* **47**, 319–346
38. El-Maghrabi, M. R., Lange, A. J., Kummel, L., and Pilkis, S. J. (1991) *J. Biol. Chem.* **266**, 2115–2120
39. Chen, B. P. C., Liang, G., Whelan, J., and Hai, T. (1994) *J. Biol. Chem.* **269**, 15819–15826
40. Schmid, E., Schmid, W., Jantzen, M., Mayer, D., Jastorff, B., and Schutz, G. (1987) *Eur. J. Biochem.* **165**, 499–506
41. Brockenbrough, J. S., Weir, G. C., and Bonner-Weir, S. (1988) *Diabetes* **37**, 232–236
42. Leahy, J. L. (1996) in *Diabetes Mellitus* (LeRoith, D., Taylor, S. I., and Olefsky, J. M., eds) pp. 103–113, Lippincott-Raven, Philadelphia
43. Anderson, T., Schein, P. S., McMenamin, M. G., and Cooney, D. A. (1974) *J. Clin. Invest.* **54**, 672–677
44. Sanfey, H., Bulkley, G. B., and Cameron, J. L. (1984) *Ann. Surg.* **200**, 405–413
45. Parks, D. A., Bulkley, G. B., and Granger, D. N. (1983) *Surgery* **94**, 428–432
46. Baynes, J. W. (1991) *Diabetes* **40**, 405–412
47. Braganza, J. M. (1988) in *Free Radicals: Chemistry, Pathology and Medicine* (Rice-Evands, C., and Dormandy, T., eds) pp. 357–381, Richelieu Press, London
48. Freeman, B. A. (1982) *Lab. Invest.* **47**, 412–426
49. Kakkar, R., Mantha, S. V., Radhi, J., and Prasad, K. (1998) *Clin. Sci.* **94**, 623–632
50. Xu, B., Moritz, J. T., and Epstein, P. N. (1999) *Free Radic. Biol. Med.* **27**, 830–837
51. Kloner, R. A., Przyklenk, K., and Whittaker, P. (1989) *Circulation* **80**, 1115–1127
52. Weir, G. C., Sharma, A., Zangen, D. H., and Bonner-Weir, S. (1997) *Acta Diabetol.* **34**, 177–184
53. Jonas, J. C., Sharma, A., Hasenkamp, W., Ilkova, H., Patané, G., Laybutt, R., Bonner-Weir, S., and Weir, G. C. (1999) *J. Biol. Chem.* **274**, 14112–14121
54. Bonner-Weir, S. (2000) *J. Mol. Endocrinol.* **24**, 297–302
55. Bouwens, L., and Klöppel, G. (1996) *Virchows Arch.* **427**, 553–560
56. Hellerström, C. (1984) *Diabetologia* **26**, 393–400
57. Bouwens, L., Wang, R. N., De Blay, E., Pipeleers, D. G., and Klöppel, G. (1994) *Diabetes* **43**, 1279–1283
58. Bouwens, L., Lu, W. G., and Krijger, R. D. (1997) *Diabetologia* **40**, 398–404
59. Eriksson, U., and Swenne, I. (1982) *Biol. Neonate* **42**, 239–248
60. Swenne, I., and Eriksson, U. (1982) *Diabetologia* **23**, 523–528
61. Timmerman, L. A., Clipstone, N. A., Ho, S. N., Northrop, J. P., and Crabtree, G. R. (1996) *Nature* **383**, 837–840
62. Timchenko, N. A., Harris, T. E., Wilde, M., Bilyeu, T. A., Burgess-Beusse, B. L., Finegold, M. J., and Darlington, G. J. (1997) *Mol. Cell. Biol.* **17**, 7353–7361
63. Timchenko, N. A., Wilde, M., and Darlington, G. J. (1999) *Mol. Cell. Biol.* **19**, 2936–2945